Low dose/dose rate γ irradiation protects *Drosophila melanogaster* chromosomes from double strand breaks and telomere fusions by modulating the expression of *Loquacious*.

Porrazzo A.[1,3], Cipressa F.[2,3], De Gregorio A. [1] , De Pittà C[4]., Sales G. [4], Morciano P.[5], Esposito G[6], Tabocchini M.A[7]., Cenci G.[1,3,*]

1. Dipartimento di Biologia e Biotecnologie "C. Darwin". Sapienza Università di Roma, Rome, Italy
2. Centro Studi e Ricerche ''Enrico Fermi'',
3. Fondazione Cenci Bolognetti/ Istituto Pasteur Italia, Rome, Italy
4. Dipartimento di Biologia, Università di Padova, Padua, Italy
5. INFN - Laboratori Nazionali del Gran Sasso,
6. Istituto Superiore di Sanita` (ISS) and INFN-Roma 1
7. INFN-Roma 1

ORCID AP 0000-0002-2914-7984
ORCID GS 0000-0003-2078-5661
ORCID GE 0000-0002-8751-1895
ORCID FC 0000-0002-9919-5295
ORCID CDP 0000-0001-8013-8162
ORCID AT 0000-0003-3244-6106
ORCID PM 0000-0002-8101-0096
ORCID GC 0000-0002-9628-1411

*Corresponding Author:
Giovanni Cenci, giovanni.cenci@uniroma1.it

Running Title: Low dose/dose rate γ irradiation and chromosome integrity

Abstract
It is still continuously debated whether the low-dose/dose-rate (LDDR) of ionizing radiation represents a hazard for humans. Model organisms, such as fruit flies, are considered valuable systems to reveal insights into this issue. We found that, in wild-type *Drosophila melanogaster* larval neuroblasts, the frequency of Chromosome Breaks (CBs), induced by acute γ-radiation, is significantly reduced when flies are previously exposed to a protracted dose of 0.4 Gy delivered at a dose rate of 2.5 mGy/h. This indicates that this exposure, which is associated with an increased expression of DNA damage response proteins, induces a radioadaptive response (RAR) that protects Drosophila from extensive DNA damage. Interestingly, the same exposure reduces the frequency of telomere fusions (TFs) from Drosophila telomere capping mutants suggesting that the LDDR can generally promote a protective response on chromatin sites that are recognized as DNA breaks. Deep RNA sequencing revealed that RAR is associated with a modulation of genes involved in RNA processing and the reduction of expression of *Loquacious D (Loqs-RD)* gene that encodes a well-conserved dsRNA binding protein required for esiRNAs biogenesis. Remarkably, loss of *Loqs* mimics the LDDR-mediated chromosome protection as it decreases the IR-induced CBs and TF frequency. Thus, our work identifies Loqs as a key factor in mediating the cellular response to LDDR and reveals that the study of the molecular bases underlying RAR is instrumental for unraveling novel and conserved epigenetic routes that have evolved to preserve genome integrity following robust insults to DNA.

Introduction

Low doses of ionizing radiation constitute one of various types of genotoxic stresses to which all living organisms are continuously exposed during their daily life. Human exposure to low-dose radiation depends on both natural (i.e. radon gas, terrestrial radiation and cosmic rays that penetrate the Earth's atmosphere) and man-made (i.e. such as X-rays, radiation used to diagnose diseases and for cancer therapy and fallout from nuclear explosives testing) sources. It has been reported that 2.4 mGy is the average dose that a person receives per year (UNSCEAR, 2008), although this may vary worldwide depending on the geographical location. Whereas there is no doubt that intermediate and high doses of ionizing radiation, delivered either acutely or during a prolonged period, have deleterious effects in humans, including, but not exclusively, cancer and developmental defects, the biological consequences at lower doses (below 100 mGy) are less clear (Morgan and Bair, 2013; Shibamoto and Nakamura, 2018). Yet, the comprehension of low doses radiation risks has societal importance considering the concerns arising from occupational radiation exposure, screening tests for cancer, nuclear power generation, frequent-flyer risks, missions in space, and radiological terrorism. Several efforts have been made to evaluate the effects of low doses/low dose rate radiation from epidemiological studies. However, these studies are influenced by several uncertainties that include, but not limited to the radiation quality, the age at exposure, the effects of both internal and external exposures, gender and temporal factors (Morgan and Bair, 2013; Shibamoto and Nakamura, 2018). Thus, to better assess the accuracy of risk estimates and increase the statistical power, the low dose epidemiological studies would require a large population to be analyzed or pooling of data from several observations.

The linear-no-threshold (LNT) model has long been used for setting dose limitations on radiation exposure, that is, basically assuming that all radiation exposures, regardless of how low the dose is, increase the risk for cancer (Council, 2006). The justification of using this model is that radiation carcinogenesis is triggered by DNA damage. Yet, the possibility of improving the LNT risk extrapolation model has been recently debated as other potential mechanisms affecting radiation carcinogenesis have been described (Calabrese, 2015, 2017; Marcus, 2016). These include epigenetic mechanisms, transmissible genome instability, bystander effects, radiation hormesis and Radio Adaptive Response (Belli and Tabocchini, 2020; Shibamoto and Nakamura, 2018).

The Radio Adaptive Response (RAR) is a protective phenomenon where a small initial low radiation dose (priming) reduces the response to a subsequent high radiation dose (challenging). The main proposed mechanisms to explain RAR are an increase of the efficiency of DNA repair activity and of the level of antioxidant enzymes (Esposito et al., 2011; Nenoi et al., 2015; Tapio and Jacob, 2007). First discovered in cultured human lymphocytes (Olivieri et al., 1984), RAR has been observed both *in vivo* and *in vitro* in several mammalian systems as well as in the zebrafish embryo model using various end points such as cellular damage, cell lethality, chromosomal aberrations, mutation induction, radio-sensitivity and DNA repair (Esposito et al., 2011; Nenoi et al., 2015). Although the general view posits that RAR may be due to enhanced repair of DNA damage in the " primed" cells (those having exposed to a priming dose) when compared to the " unprimed" cells, several experiments using different cell types and irradiation procedures produced conflicting results (Stecca and Gerber, 1998). Thus our understanding on the molecular mechanisms that underlie RAR is still elusive. Indeed, the manifestation of the response depends on several factors such as the cell, tissue, animal types, genetic background, p53 status. Moreover, the dose, dose rate and time period between priming and challenging dose may be crucial for a cell to induce RAR. It is still unclear what dose and dose rate might trigger RAR in humans (Shibamoto and

Nakamura, 2018; Tapio and Jacob, 2007). This is also complicated by the high degree of inter-individual variation, which in turn depends on the radio-sensitivity of an individual. Thus, the evaluation of whether low radiation doses or dose rates represent a risk estimate factor for radiation protection purposes requires a better understanding of the RAR.

Recently, a link between radioprotection and telomere maintenance has emerged. The examination of leukocytes in atomic bomb survivors of Hiroshima revealed a long-term detrimental effect of an inverse correlation between telomere length and IR dose (Lustig et al., 2016). Effects on telomere length have also been observed during space mission as cosmic radiation has been shown to elongate telomeres. Interestingly, two days on the Earth restored normal telomere length indicating that elongation of telomeres can be considered as a well-established adaptive response to high radiation levels in space (Luxton et al., 2020a; Luxton et al., 2020b). Nevertheless, exposure to high radiation background does not affect telomere length suggesting the existence of a well-defined threshold under which the effects of radiation exposure are undetectable (Das et al., 2009; Movahedi et al., 2019).

Here we show that Drosophila larvae that are chronically exposed to a specific priming γ-radiation dose of 0.4 Gy delivered at 2.5 mGy/h (0.4 Gy LDDR) during embryo-to-third instar larvae development, exhibit a strong reduction of chromosome break frequency after either a 10 Gy γ ray challenging dose or treatment with the radiomimetic agent bleomycin, with respect to non-pretreated flies. Moreover, we demonstrate that the same LDDR treatment reduces the frequency of telomeric fusions (TFs) associated with the loss of telomere capping suggesting that the 0.4 Gy LDDR-mediated protective effect can be generally extended to chromatin sites that are also inappropriately recognized as DNA breaks. Deep RNA sequencing indicates that the 0.4 Gy LDDR-mediated protective effect on chromosome breaks is associated with a reduction of the Loquacious D (Loqs-PD) isoform, a well conserved dsRNA binding protein required for the esiRNA biogenesis. Interestingly, loss of Loqs PD (but not of other isoforms) reduces IR-induced DSBs and TFs indicating that modulation of Loqs PD may represent an escape route for the cell to preserve chromosome integrity upon induction of genotoxic stress.

Results

Identification of specific low dose/dose rate values that protect Drosophila chromosomes from ionizing radiation-induced Double Strand Breaks (DSBs)

To investigate the effects of low dose/dose rate irradiation on DNA damage, we carried out a pilot experiment to verify whether a pretreatment with chronic low doses of γ rays (priming dose) affects the frequency of total chromosome breaks (CBs) induced by an acute γ dose of 10 Gy (challenging dose) in Drosophila third instar larvae neuroblasts. Vials containing 12 h Drosophila embryos were placed at 23 °C inside the LIBIS irradiation facility (Esposito et al., 2016) and irradiated continuously at dose rates of 1.4, 2.5 and 4.4 mGy/h until they developed into third instar larvae (7 days). To obtain these dose rates, the vials were placed simultaneously inside the LIBIS irradiator at three distances, namely: d_1= 100 cm (for 1.4 mGy/h), d_2=74 cm (for 2.5 mGy/h) and d_3=56 cm (for 4.3 mGy/h), from a Cs-137 source with activity of 17.6 GBq (at August 24, 2012) (Figure 1). Control non-pretreated vials were kept in parallel outside the LIBIS. The third instar larvae populate the vials from about the fourth day (89 h) up to about the seventh day (161 h) after the start of chronic irradiation. To select larvae that received a total of 0.1 Gy (1.4 mGy/h), 0.2 Gy (2.5 mGy/h) or 0.4 Gy (4.3 mGy/h) priming dose, vials were irradiated for 89 h at the distance of d_1, d_2 and d_3, respectively (Figure 1a). We have also collected larvae coming out after 161 h of maintenance at LIBIS at d_1, d_2 and d_3, distances that resulted into a final exposure of 0.2 Gy (1.4 mGy/h), 0.4 Gy (2.5 mGy/h) and 0.7 Gy (4.3 mGy/h), respectively (Figure1). Irradiated and non-irradiated control vials were then exposed to an acute γ dose of 10 Gy (challenging dose) at the dose rate of about 0.7 Gy/min and four hours later larvae were dissected for the analysis of CBs frequency in neuroblasts. The average number of total chromosome breaks per cell (CBs/Cell) was calculated by measuring the ratio of the total number of chromatid deletions (CDs, scored as a single event) and isochromosome breaks (ISOs or chromosome deletions, scored as two events) to the total number of metaphases (Figure 2b). Figure 1c shows the CBs/Cell frequency induced by the challenging dose of 10 Gy plotted as a function of the priming dose for different priming dose rates (we counted at least 300 cells for each dose/dose rate combination). The comparison between pre-irradiated and non pre-irradiated larvae revealed that the frequency of CBs induced by the challenging dose was significantly reduced in larvae that were exposed to a priming dose of 0.7 Gy (4.3 mGy/h; 23%) and 0.4 Gy (2.5 mGy/h; 35%). However, we found that the priming dose of 0.1 Gy (1.4 mGy/h), 0.2 Gy (1.4 mGy/h) and 0.2 Gy (2.5 mGy/h) and 0.4 Gy (4.3 mGy/h) did not modify significantly the average number of total CBs/cell induced by the challenging dose (Figure 1c). Overall, these results strongly suggest that the low dose/dose rate irradiation, delivered at a specific time frame, is able to trigger a RAR to DNA damage induction in Drosophila larval mitotic cells. Given that the 0.4 Gy (2.5mGy/h) priming dose yielded the strongest CBs reductions, we decided to focus on this experimental condition (hereafter 0.4 Gy LDDR) to further investigate the mechanisms underlying the RAR.

Cytological Characterization of a RAR in Drosophila neuroblasts.

To get insights into the reduction of frequency of CBs induced by the 0.4 Gy LDDR, we analyzed ~ 1000 DAPI-stained colchicine treated neuroblast metaphases from both pretreated and non-pretreated third instar larvae exposed to the 10 Gy challenging dose (Figure 2). Chromosomes were fixed at 4h and 8h post irradiation time points (PIR) to recover cells that were irradiated in the S-G_2 or G_1 stage, respectively (Gatti et al., 1974). We found that in non-pretreated larvae the average number of CBs/Cells induced by the challenging dose was ~1.0 and ~ 0.8 in females and males, respectively after 4hPIR. In agreement with our pilot experiment, the 0.4 Gy LDDR determined a ~2 fold decrease of

CBs/Cells frequency in both male and female larval neuroblasts. In particular, in both sexes the relative proportions of CDs (~20% and ~15%), did not significantly change with respect to those (~30% and ~16%) of non-pretreated females and males, respectively. In contrast the frequency of ISOs (~20% and 16%) in treated females and males, respectively was significantly reduced compared to those of non-pretreated females and males (~39% and ~33%, respectively) suggesting that RAR preferentially acts on preventing chromosome-type breaks. We have also measured the frequency of heterochromatic breaks occurring at the pericentric regions of autosomes and X chromosomes as well as on the Y chromosomes. In this case we also found no significant differences in the proportion of heterochromatic breaks between 0.4 Gy LDDR treated (~9%) and non-pretreated larvae (~10%) in both sexes. Taken together, these analyses show that 0.4 Gy LDDR treatment renders neuroblast chromosomes resistant to IR-induced DNA breakage at both euchromatin and heterochromatin sites (Supplementary Table1).

We sought to understand whether the 0.4 Gy LDDR could affect CBs frequency also at 8h PIR, when cells are irradiated during the G_1 stage. The analysis of ~1000 female metaphases revealed no statistically significant difference on CBs frequency between non-pre-treated (53%) and 0.4 Gy LDDR treated (45%) larvae at 8hPIR (Figure 2a). This suggests that 0.4 Gy LDDR could primarily influences the HR-based repair systems that, by employing sister chromatids as templated DNA synthesis to regenerate the sequence surrounding the break site, is restricted to S-G_2 phase (Hart et al., 2017).

We finally evaluated whether the radio-resistance could be also maintained for more than one generation. Thus, male and female adult flies that developed from 0.4 Gy LDDR-pretreated larvae were mated to each other outside the LIBIS and the resulting F_1 larvae irradiated with 10 Gy. Interestingly, we found that the frequency of CBs, calculated at 4hrPIR was ~2 fold reduced in metaphases from both male and female F_1 larvae of 0.4 Gy LDDR -derived adult parents (n=~800 for both sexes) with respect to control F_1 larvae deriving from non-pretreated adults (Figure 2a). This indicates that the RAR shows a transgenerational inheritance.

To analyze whether the 0.4 Gy LDDR affected the regulation of G_2/M checkpoint, we carried out a standard checkpoint assay evaluating the proportion of dividing cells (Mitotic Index, MI) in larval brain cells fixed at different times after the challenging dose (10 Gy). As shown in Figure 3a, the MI of the non-pretreated Oregon R control brains dropped at 5–30 min PIR, remained low for 1 h and came back to a normal value only at 2 h PIR. The MI of 0.4 Gy LDDR -pretreated larvae decreased as much as in control brains at 5-30 min PIR, but then markedly increased after 30 min PIR suggesting that the 0.4 Gy LDDR exposure determined a faster recovery from the G_2-M checkpoint (Figure 3a) compared to non-pretreated cells, very likely due to a reduced amount of DNA damage (~50%) to be repaired.

We also checked whether the rate of IR-induced apoptosis was influenced by the 0.4 Gy LDDR. Immunostaining of whole-mounted brains and imaginal discs for cleaved-Caspase-3 revealed that numbers of cleaved-Caspase 3 positive cells in treated larval brains was indistinguishable from that observed in non-pretreated control after the challenging dose, indicating that the RAR does not reduce the occurrence and distribution of apoptosis caused by extensive DNA damage (Supplementary Figure 1). We finally compared the occurrence of DNA replication in non-pretreated and pretreated brain cells by analyzing the incorporation of the EdU (5-ethynyl-2'-deoxyuridine) analog of thymidine, before and after IR (see Materials and Methods). Before 10 Gy irradiation, non-pretreated wild-type and 0.4 Gy LDDR-pretreated larvae, exhibited a similar proportion of nuclei (~14%; n= ~2000 cells) that were actively replicating their DNA and incorporated EdU. However, after irradiation, whereas in non-pretreated wild-type brains the frequency of

EdU-labeled nuclei dropped to 6.5% (as a consequence of the arrest of S phase), 0.4 Gy LDDR-pretreated brains displayed a proportion of positive nuclei (~20%; n= ~2000 cells) very similar to unirradiated larvae (Figure 3c). Based on incorporation pattern of EdU, according to Cenci et al., 2015 (Cenci et al., 2015), we subdivided the S phase in three subclasses, namely S_1 (early/mid S; nucleus partially or completely stained with the exception of the chromocenter), S_2 (mid/late S; staining at the chromocenter and at a less compacted nuclear area) and S_3 (late S; only chromocenter stained; (Figure 3b). This classification revealed us that pretreated and non-pretreated cells did not differ in the relative frequencies of nuclei showing S_1, S_2 and S_3 EdU incorporation patterns (Figure 3d). Altogether, these results indicate that 0.4 Gy LDDR-pretreated cells recover much faster than non-pretreated controls from the DNA damage-induced replication block.

The Radio Adaptive Response to DSBs relies on a more efficient DNA damage response

To determine whether the reduction of chromosome breaks promoted by 0.4 Gy LDDR depends on the presence of proteins required for specific DSB repair pathways, we checked whether 0.4 Gy LDDR-pretreated larvae bearing mutations in genes encoding DSB repair master proteins (dATM, dRad50, dNbs1, dMre11), HR-specific repair proteins required for resection or homology search and strand invasion (dRad51), and NHEJ-specific proteins (ligase IV) elicited a decrease frequency of chromosome breaks after the challenging dose. The analysis of mitotic chromosomes from all mutants revealed no significant difference ($p<0.05$) in the frequency of CBs between 0.4 Gy LDDR-pretreated and non-pretreated larvae indicating that the 0.4 Gy LDDR-mediated resistance to γ-ray-induced CBs is strictly dependent on DNA repair genes (Figure 3e).

We then verified whether 0.4 Gy LDDR affects the kinetics of γH2Av recruitment to chromatin breaks. H2Av is the functional homolog of H2AX in Drosophila and its phosphorylation at Ser147 is induced by DSB (Madigan et al., 2002). 0.4 Gy LDDR -pretreated and non-pretreated larvae were exposed to 10Gy γ rays and then checked by IF for the presence of γH2Av foci in brain mitotic cells after 5 min, 15 min, 30 min and 60 min PIR. We found that in non-pretreated control larval brains, the number of γH2Av foci/cell progressively increased over the time, reached the highest peak (6 foci/cell) at 30 min PIR and started to slowly decrease at 60 min PIR (Figure 4b). LDDR -pretreated neuroblasts also showed a progressive increment of the γH2Av foci/cell frequency over the time with a peak at 30 min PIR. Interestingly the average of foci/cell at 30 min was around ~4 indicating that, differently from non-pretreated controls, LDDR-pretreated brains accumulate less damage very likely as the results of either an accelerated DNA damage response or a more efficient repair (Figure 4b). We have also analyzed the kinetics of γH2Av accumulation by WB and found that, consistently with our IF results, at 30 min PIR γH2AV in 0.4 Gy LDDR-pretreated cells does not accumulate as robustly as in non-pretreated cells (Figure 4c, d) confirming that 0.4 Gy LDDR could accelerate the completion of DNA damage response. It is worth noting that the amount on DNA damage right after irradiation (5 min PIR) as revealed by the levels of γH2AV in 0.4 Gy LDDR-pretreated cells is comparable to that of non-pretreated cells suggesting that in both conditions chromatin is similarly sensitive to the induction of DNA breaks. We finally analyzed the levels of the MRN complex and found a statistically significant increase of Rad50 and Nbs1 protein levels in 0.4 Gy LDDR-pretreated cells with respect to non-pretreated cells (Figure 4e, f). Collectively these data, along with the genetic analyses indicating a strict requirement of DNA repair genes, suggest that the RAR relies on an efficient DNA damage response. However, we cannot rule out the possibility that the LDDR could also influence chromatin compaction making it more reluctant to damage compared to non-pretreated chromatin.

LDDR protects chromosomes from different genotoxic insults and dysfunctional telomeres

We also asked whether LDDR treatment reduces chromosome breaks induced by other mechanisms beyond ionizing radiation. We thus treated larval brains with different concentration of cisplatin, urea and bleomycin, three well known radiomimetic compounds that induce chromosome breaks in mammalian cells. Whereas we failed to obtain broken mitotic chromosomes upon treatment with either cisplatin or urea, the incubation of larval brain with 500 µg/ml bleomycin induced frequent CBs (0.61 CB/cell; n= 136), indicating that this molecule triggers DSBs also in Drosophila neuroblasts (Supplementary Table 2). Interestingly, we observed that this CBs frequency significantly dropped to 0.33 CB/cell (n= 324) in metaphase chromosomes from 0.4 Gy LDDR-pretreated larvae (Supplementary Table 2), indicating that LDDR is able to protect Drosophila genome from breakage induced by different genotoxic insults.

This finding prompted us to check whether other DNA damage-induced events are also affected by LDDR. We focused on DNA damage response elicited by dysfunctional telomeres and verified the occurrence of telomere fusions (TFs) in mutants with a defective telomere capping. Depletion of either terminin complex components and or terminin-associated factors induces the formation of multicentric linear and ring chromosomes very likely because of HR- or NHEJ-mediated fusion events that occur at uncapped telomeres (Cacchione et al., 2020; Raffa et al., 2011) (for examples of TFs see Figure 5a). We thus measured the frequency of TFs of 0.4 Gy LDDR-pretreated mutants in selected genes encoding terminin proteins (*verrocchio (ver)*, and HOAP-encoding *caravaggio (cav*)) and terminin associated factors (HP1a, Pendolino (Peo) and Effete/UbcD1 (Eff)). As indicated in Figure 5b, we found that in all mutants analyzed, 0.4 Gy LDDR yielded a significant reduction of TFs indicating that this exposure exerts a protective effect at uncapped chromosome ends. We have also analyzed the frequency of TFs caused by mutations in *tefu, nbs, rad50* and *mre11* genes encoding for the DNA repair factors ATM, Nbs, Rad50 and Mre11, respectively and which are also required for protecting telomeres from fusion events (Cenci, 2009; Cipressa and Cenci, 2013). Interestingly we found that the frequency of TFs in DNA repair mutants was indistinguishable from that of non-pretreated mutants (Figure 5b) indicating that, similarly to RAR, the 0.4 Gy LDDR-induced telomere protection depends on DNA repair factors. However, the reduction of TFs did not always correlate with a reduction of γH2Av-positive Telomere Induced Foci (TIF) indicating that, unlike chromosomal DSBs, the reduction of fusigenic feature or uncapped telomeres has not a direct effect on the cytological detection of telomere damage (Supplementary Figure 2a,b). We finally checked if LDDR could induce an increase of retro-transposition of the telomeric retroelement HeT-A, as it occurred in flies that were chronically exposed to sub-lethal doses of paraquat (Korandova et al., 2018). RT-qPCR analysis revealed no differences in the HeT-A expression between non-pretreated and 0.4 Gy LDDR treated TF mutants (Supplementary Figure 2c), indicating that the 0.4 Gy LDDR protective effects on uncapped telomeres is unlikely due to an adaptive role of telomere elongation against the loss of capping.

Differential Gene Expression and Genetic Analyses reveal Loquacious (Loqs) as a RAR responsive factor.

To assess whether the 0.4 Gy LDDR RAR was accompanied by differential modulation of specific set of genes, we performed a genome wide RNA-seq analysis of total RNAs extracted from unirradiated (A), 10Gy- (B), 0.4 Gy LDDR- (C) and 0.4 Gy LDDR + 10 Gy-irradiated (D) larval male brains. To search for gene functions specifically associated to the

chromosome break phenotype, RNAs of 10 Gy- and 0.4 Gy LDDR + 10 Gy irradiated larvae were extracted from brains dissected after 4 h following the acute dose exposure. Pairwise comparisons revealed that the 0.4 Gy LDDR treatment *per se* has not determined a statistically significant transcription modulation with respect to the unirradiated condition. In contrast, both 10Gy- and 0.4 Gy LDDR + 10 Gy-treatments determined a moderate, yet statistically significant, modulation of transcription in all comparisons (see Supplementary Tables 4-8 for a list of both upregulated and downregulated genes). The Venn diagram including all differentially expressed genes (DEGs) from 0.4 Gy LDDR + 10 Gy *vs.* 10 Gy, 0.4 Gy LDDR + 10 Gy *vs*. 0.4 Gy LDDR and 10Gy *vs*. 0.4 Gy LDDR comparisons, has shown that only a very low percentage of genes were in common among all comparisons (Figure 6a). This indicates that our RNA-seq analysis has indeed revealed modulation of specific genes in all conditions tested. To further identify genes potentially involved in the RAR, we focused on the set of DEGs found in the 0.4 Gy LDDR + 10 Gy *vs*. 10 Gy comparison (D *vs*. B). DAVID functional enrichment analysis (EASE score < 0.05, Adjusted p-value <0.05) revealed that the DEGs from this comparison are involved in RNA processing. The corresponding modulation of these 18 genes is indicated in the Heat Map of Figure 6b. 3 genes *(l(3)72Ab, CG5205 and CG8064)* were also differentially expressed in the 0.4 Gy LDDR + 10 Gy vs 0.4 LDDR Gy comparison. We named the remaining genes, which were unique of the 0.4 Gy LDDR + 10 Gy *vs*. 10 Gy comparison, Radio Adaptive Responsive Genes (RARGs).

Among RARGs, we have drawn our attention to the modulation of *loqs (loquacious)* transcripts that encode a dsRNA binding protein required for siRNA and micro-RNA biogenesis (Marques et al., 2010; Zhou et al., 2009). Four different transcripts have been identified for *loqs* (*loqs-RA*, *loqs-RB, loqs-RC* and *loqs-RD)* that give rise to the Loqs-PA, Loqs-PB, Loqs -PC and Loqs –PD isoforms, respectively. Loqs-PA and Loqs-PB, which are the fly homologs of TRBP, interact with Dcr-1 during miRNA biogenesis (Hartig et al., 2009; Lim et al., 2016; Saito et al., 2005; Zhou et al., 2009). Loqs-PC is rarely expressed and has no known function (Zhou et al., 2009) while Loqs-PD facilitates Dcr-2–dependent endosiRNA biogenesis (Lim et al., 2016; Zhou et al., 2009). Our RNA-Seq experiment showed that the *loqs-RD* (but not the other transcripts) appeared ~2 fold decreased in 0.4 Gy LDDR + 10 Gy-pretreated samples compared to 10 Gy irradiated samples. This reduction was also validated by RT-qPCR on three independent RNA extractions (Figure 7a) suggesting that LDDR could specifically influence Loqs-dependent biological processes.

To further understand whether the reduction of Loqs indeed accounts for the RAR, we analyzed chromosome integrity in chronically irradiated Loqs-depleted larval brain cells with and without the 0.4 Gy LDDR-treatment. We thus measured the frequencies of CBs in the $loqs^{KO}$ null mutant upon 0.4 Gy LDDR, 10Gy and 0.4 Gy LDDR +10Gy treatments as well as in unirradiated $loqs^{KO}$ brains using the same experimental set up described above. Intriguingly, we found that while unirradiated $loqs^{KO}$ larval brain cells exhibited very rare CBs, the frequency of CBs in this mutant was >50% reduced with respect to OR-R control larvae (n= 250) after the exposure to 10 Gy (Figure 7b). This suggests that the depletion of Loqs could mimic the effect of the 0.4 Gy LDDR priming dose in determining resistance to ionizing radiation-induced CBs. Interestingly we observed that this response was lost when Loqs-PD, but not –PB, was expressed in the $loqs^{KO}$ null mutant (Figure 7b) confirming that the reduction only of this specific isoform is involved in triggering radio-resistance to CBs. However, we observed that the >50% reduction of CB frequency in 10 Gy irradiated $loqs^{KO}$ null mutant, did not further decrease upon the 0.4 Gy LDDR pretreatment suggesting that the effect of loss of Loqs on the radio-resistance is epistatic over the 0.4 Gy (2.5 mGy/h) LDDR priming dose (Figure 7b). Finally, we observed a ~50% reduction of CBs also in $loqs^{KO}$/+ heterozygotes suggesting that radioresistance effect is

dominant and confirming our RNA-seq data that even a moderate downregulation of this gene can account for the protection against extensive DNA breakage.

To confirm that the loss of Loqs mirrors the effects of the 0.4 Gy LDDR -induced radio-resistance, we first verified whether the response to CBs in Loqs-depleted cells is also dependent on DNA repair factors. We thus sought to analyze CB frequency in *loqs*^{KO}*; tefu*^{atm} and *loqs*^{KO}*; nbs*^{1} double mutants. While *loqs*^{KO}*; tefu*^{atm} double mutants turned out to be early lethal thus preventing us for a further characterization, we found that the frequency of CBs in 2 Gy irradiated *loqs*^{KO}*; nbs*^{1} larvae was similar to that of 2 Gy irradiated *nbs*^{1} single mutants (Supplementary Table 3) confirming that the protection from chromosome breakage in Loqs-depleted and 0.4 Gy LDDR cells requires shared DNA protein factors. Finally, we observed that the kinetics of γH2Av recruitment in *loqs*^{KO} and in 0.4Gy LDDR + 10 Gy cells, were similar (Figure 7c). Altogether, this set of evidences confirm that repression of Loqs explains the LDDR-mediated RAR and endorses the view that Loqs-PD is *a bona fide* a low dose responsive gene.

Loss of Loqs reduces the frequency of Telomere Fusions in Drosophila telomere capping mutants.

We then sought to verify if Loqs, similarly to LDDR, affects the fusigenic ability of chromosomes with defective telomere capping. We thus checked the frequency of TFs in double mutant combinations between *loqs*^{KO} and TF mutants (*ver*^{1}*, cav*^{1}*, nbs*^{1}*)* mapping on the third chromosome and therefore more suitable for recombination with *loqs*^{KO}, located on the second chromosome. Very interestingly, we found that in *loqs*^{KO} *; ver*^{1} and *loqs*^{KO} *; cav*^{1} mutant combinations the percentage of TFs/cell was significantly lower than that observed in the corresponding controls, while, as expected TF frequency of *nbs1* mutants was not affected by loss of Loqs (Figure 7d). This finding further confirms that, similarly to RAR, the reduction Loqs is also involved in the protection of uncapped telomeres.

Discussion

We showed for the first time that a protracted exposure to the 0.4 Gy LDDR protects Drosophila chromosomes from IR- and bleomycin-induced DSBs, and from the formation of TFs as a consequence of loss of capping. Small deviations from this dose/dose rate combination either do not elicit a significant effect or reduce the number of γ-ray induced DSBs only marginally indicating that the most protective action against DNA damage requires a fine balance between dose and dose rate. Although a protective effect of low IR dose has been already observed in *Drosophila*, it was primarily associated to changes of life span upon acute irradiation (Seong et al., 2011; Zhikrevetskaya et al., 2015). Our findings have shown for the first time the contribution of LDDR to promoting a more efficient HR-dependent repair in fruit flies that enhances the DNA damage response.

Interestingly, we demonstrated that LDDR reduces also the frequency of TFs of *Drosophila* capping mutants, revealing an unprecedented protective effect on dysfunctional chromosome ends. Since Drosophila has recently emerged as a model organism for human telomere biology (Cacchione et al., 2020; Cenci et al., 2005), we can envisage that our findings could provide a valid countermeasure to inhibit telomere fusions in cancer cells. It can be argued that the reduction of TFs mediated by the 0.4 Gy LDDR, which enhances DNA repair, could appear in contradiction with the evidence that telomeres normally avoid unwanted DNA repair (Doksani and de Lange, 2014). However, it is also known that DNA repair proteins interact with telomere capping proteins to establish a protective structure during G_2-M (Doksani and de Lange, 2014; Slijepcevic, 2006; Verdun and Karlseder, 2006). We can thus hypothesize that the 0.4 Gy LDDR could reinforce the DNA repair protein recruitment that has been impaired by the loss of capping factors, thus counteracting telomere dysfunction/fusions. The findings that some Drosophila capping proteins indeed interact with the MRN complex (Bosso et al., 2019; On et al., 2021) and that loss of either ATM or MRN induces TFs (Cenci et al., 2005), gives further support to this hypothesis. Interestingly, the observation that the frequency of TFs associated to depletion of either ATM or MRN is not affected by 0.4 Gy LDDR provides a robust evidence that, similarly to the RAR, the protective effect on uncapped telomeres is dependent on the activation of DNA-damage response. Thus our results indicate that the protective effects of LDDR on CBs and TFs share common molecular bases.

Our total RNA seq analyses revealed that mRNA profile of “primed” cells is undistinguishable from that of “unprimed” cells before the induction of DSBs indicating that the 0.4 Gy LDDR *per se* has no effect on gene expression. However, we cannot exclude that LDDR could change the expression of small non-coding RNAs such as microRNAs. Furthermore, 0.4 Gy LDDR does not seem to affect life parameters as 0.4 Gy LDDR pretreated flies are fertile and do not exhibit changes in the life span (Supplementary Figure 3). However, compared to unprimed cells, the induction of DSBs in primed cells yielded a discrete modulation of gene transcription, which might help understand the molecular bases underlying the LDDR protective effects. Our evidence that the downregulation of *loqs-RD* transcript is required to prevent extensive chromosome breakage in primed cells could suggest a link between esiRNAs biogenesis and radio adaptive response. Remarkably, we found that depletion of *loqs-RD,* similarly to 0.4 Gy LDDR, confers radio-resistance to mitotic chromosomes upon DSBs induction, confirming that the downregulation of this dsRNA binding protein can account for the 0.4 Gy LDDR-mediated response to DNA damage. In light of this, we can certainly state that *loqs-RD* can be considered the first 0.4 Gy LDDR-responsive gene ever characterized. In addition, we would like to point out that an understanding of the molecular basis of RAR could help identify unanticipated factors involved in radioresistance.

Loqs-PD interacts with Dicer-2 through its C-terminal region, and is crucial for

efficient production of subset of siRNAs, namely hairpin-derived endo-siRNA, cis-Natural Antisense Transcript (NAT)-derived endo-siRNA, as well as exo-siRNAs generated from an inverted repeat transgene (Fukunaga et al., 2012). However, Loqs-PD is not essential for the production of transposon-derived endo-siRNAs and virus-derived exo-siRNAs (Marques et al., 2013). Locus-specific siRNA formation has been observed associated to DSBs in different systems, including flies (Francia et al., 2012; Michalik et al., 2012; Wei et al., 2012) and promoting repair by HR in mammalian cells and plants (Gao et al., 2014; Wei et al., 2012). However, as the inactivation of siRNA pathways does not result in DNA repair defects in flies, the significance of siRNA formation in Drosophila DNA repair remains unaddressed (Malone and Hannon, 2009). Thus it is plausible to consider that endogenous siRNAs derived from cis-antisense transcripts as well as from other dsRNA sources that are normally converted to siRNA by Loqs-PD, do not play a direct role in DNA repair thus explaining why *loqs* mutants do not elicit defects in DNA repair. We like to speculate that the LDDR-induced *loqs-RD* downregulation could determine an enrichment of cis NATs that are known to favor a more competent activity of DNA repair machinery (Keskin et al., 2016; Keskin et al., 2014). In addition cis NATs can promote chromatin remodeling and resolution of R-loops, including the telomeric ones (Faghihi and Wahlestedt, 2009). Thus, cis NATs accumulation could represent the shared molecular mechanism between reduction of CBs and protection from TFs. Further investigations will shed some lights on this issue. Given the high level of homology between Loqs-PD and its human counterpart TARBP/PACT, it would be extremely interesting to evaluate in the future whether TARBP/PACT could also induce protective effects on human chromosomes.

Materials and Methods

Drosophila strains

The mutations in DNA repair genes *mei41*^{29D}, *rad50*$^{\Delta 5.1}$, *mre11*^{DC}, *nbs*^{1}, *tefu*^{atm6} and in telomere capping genes *cav*^{1}, *moi*^{1}, *ver*^{1}, *Su(var)205*^{05}, *eff*^{tre2}, *peo*^{h}, and *peo*^{1} were previously described (Cenci et al., 2015; Cenci et al., 1997; Cenci et al., 2003; Ciapponi et al., 2004; Ciapponi et al., 2006; Laurencon et al., 2003; Raffa et al., 2010; Raffa et al., 2009; Silva et al., 2004) The mutant stocks *lig4*^{5} (Bl#8519), *rad51*^{1}*/SpnA1* (Bl#3322), and *loqs*^{KO} (Bl#65411) were obtained from the Bloomington Stock Center. The *loqs*^{KO} ; *[loqs-PA]*, *loqs*^{KO} ; *[loqs-PB]* and *loqs*^{KO} ; *[loqs-PD]* lines were a generous gift from P. Zamore (University of Massachusetts Medical School, Worcester, MA). The *Oregon* R strain was used as a control in all experiments. All strains were maintained at 25 °C on *Drosophila* medium (Nutri-Fly®GF; Genesee Scientific) treated with propionic acid. The detailed information on the balancers and the genetic markers used are available online on Flybase (http://flybase.bio.indiana.edu/).

Irradiation treatments

All the irradiation exposures were carried out at the Istituto Superiore di Sanità (ISS). For the chronic γ ray treatment 12 hours embryos from 20 young females mated to 20 young males were irradiated in the LIBIS γ-irradiation facility (^{137}Cs sources; Eckert & Ziegler Nuclitec GmbH, Braunschweig, Germany) (Esposito et al., 2016). The 0.4 Gy LDDR priming dose was chronically delivered with a dose rate of 2.5 mGy/h during embryo to third instar development (7 days at 25°C). For the RAR analysis, chronically exposed third instar larvae were irradiated with 10 Gy γ rays (challenge dose) from ^{137}Cs sources, at a dose rate of 0.7 Gy/min using the Gammacell Exactor 40 (Nordion). Following irradiation, non-irradiated and irradiated flies were maintained in the same incubator at 25°C.

Bleomycin treatment

Bleomycin treatment was performed on third instar larval brains. *Drosophila* brains were dissected in 1X PBS (Phosphate Buffered Saline), treated with 10^{-6} M colchicine for 1.5 hours and then incubated with 500 μg/ml bleomycin sulfate (European Pharmacopoeia Reference Standard) solution diluted in PBS for 15 minutes. The bleomycin-induced chromosome aberrations were evaluated by standard chromosome cytology (see below).

Chromosome cytology and microscopy

DAPI (4,6-diamidino-2-phenylindole)-stained, colchicine-pretreated *Drosophila* larval brain chromosome preparations for the analysis of chromosome aberration and telomere fusions were obtained as previously described (Cenci et al., 2003). Briefly, larval brains were dissected in NaCl 0.7% and treated for 1 hour with 10^{-6} M colchicine. Successively, they were transferred in a hypotonic solution (0.5% sodium citrate), and then they were fixed in 45% acid acetic, squashed on the slides, and immediately frozen in liquid nitrogen. After the removal of coverslips, the slides were stained with DAPI/VECTASHIELD® (VECTOR Laboratories). At least 150 metaphases for each condition were analyzed through direct observation using the inverted fluorescence microscope Nikon TE 2000 (Nikon Instruments Inc., Americas) equipped with a Charged-Coupled Device (CCD camera; Photometrics CoolSnap HQ).

Immunostaining and γH2Av foci detection

To evaluate the IR-induced γH2Av foci kinetics of recruitment to DNA damage sites, brains from irradiated third instar larvae were dissected and fixed at various post-irradiation times (PIR). The samples were incubated in 3.7% formaldehyde for 5 minutes, transferred for 30

seconds in 45% acetic acid, and fixed in 65% acetic acid. Successively, the brains were squashed and frozen in liquid nitrogen. After the removal of the coverslips, the slides were placed in cold ethanol for 15 minutes, rinsed for 15 minutes in 0.1%TritonX-100/PBS (PBT), and incubated with the anti-γH2Av primary antibody diluted in PBT (1:10; Mouse; Developmental Studies Hybridoma Bank, IA 52242) overnight at 4°C. Then, all slides were incubated with the fluorescein (FITC)-conjugated AffiniPure Donkey Anti-Mouse IgG (H+L) (1:150; Jackson ImmunoResearch) for 1 hour at room temperature (RT). Immunostained preparations were mounted in VECTASHIELD® Antifade Mounting Medium containing DAPI (4,6 diamidino-2-phenylindole) (VECTOR Laboratories). To quantify the foci at least 1000 cells were analyzed for each PIR. The slides were analyzed using a Zeiss Axioplan epifluorescence microscope (Carl Zeiss, Obezkochen, Germany) equipped with a cooled CCD camera (Photometrics, Woburn, MA, USA). The digital images in grayscale were acquired separately, converted in photoshop format, RGB stained, and merged.

EdU incorporation and staining

EdU labeling was performed as previously described (Cenci et al., 2015) using the ClickiT Alexa Fluor 488 Imaging kit (Invitrogen). Brains of third instar larvae were treated with 10 mM EdU for 60 minutes and then fixed and analyzed as described above. To quantify the EdU-positive cells, at least 2000 cells were analyzed for each condition. For the statistical analysis, two different experiments were performed.

Apoptosis levels analysis

Wings imaginal discs and brains were dissected from third instar *Oregon*-R larvae in NaCl 0.7% after 8-10 hours following the acute exposure with 10 Gy. The samples were placed in 4% formaldehyde diluted in PBS 1X for 20 minutes and then permeabilized in 1%Triton-100/PBS for 15 minutes. The samples were incubated with the anti-Cleaved *Drosophila* Dcp-1 (1:50; Rabbit; Asp216 #9578; Cell Signaling Technology®) overnight at 4°C. The next day, the slides were incubated with the AlexaFluor® 488 AffiniPure Donkey Anti-Rabbit IgG (H+L) (1:300; Jackson ImmunoResearch) for 30 minutes After a further wash of 15 minutes in PBT, the samples were stained with DAPI and mounted on the slides. The slides were analyzed using the inverted fluorescence microscope Nikon TE 2000 (Nikon Instruments Inc., Americas) equipped with a Charged-Coupled Device (CCD camera; Photometrics CoolSnap HQ). The digital images in grayscale were acquired separately, converted in photoshop format, RGB stained, and merged. The analysis of digital pictures was performed using ImageJ 1.8.0 (Image Processing and Analysis in Java).

Protein extracts and Western blotting

Protein extracts from Drosophila larval brains were obtained by dissecting 10 larval brains in 0.7% NaCl and homogenizing them in 20 μl of 2X Laemmli buffer. Protein samples were loaded into a 4-20% Mini-PROTEAN TGX precast gel to perform electrophoresis (SDS-PAGE) and blotted using the Trans-Blot® Turbo™ Transfer System on a nitrocellulose membrane (Hybond ECL, Amersham). Filters were blocked in 5% non-fat dry milk dissolved in 0.1% Tween-20/PBS for 30 min at RT and, then, incubated with anti-Giotto (1:5000; Rabbit; (Giansanti et al., 2006)) and anti-γH2Av (1:1000; Mouse; Developmental Studies Hybridoma Bank, IA 52242) overnight at 4°C. The membranes were then incubated with HRP-conjugated anti-Mouse and anti-Rabbit IgGs secondary antibody (1:5000; Amersham) for 1 hour at RT and then washed again 3 times with 0.1%Tween-20/PBS. The chemiluminescent signal was revealed through either SuperSignal™ West Femto or SuperSignal™ West Pico substrate (Thermo Scientific™) using the ChemiDoc scanning system (Bio-Rad). Band intensities were quantified by densitometric analysis

using the Image Lab 4.0.1 software (Bio-Rad). WB was repeated independently at least three times.

Genomic DNA extraction and RT-qPCR
To evaluate *Het-A* abundance, DNA was extracted from third instar larvae by standard procedures. The amount of *Het-A* was assessed by RT-qPCR using the following primers:

*Het-A*_FW 5'-ACCATAATGCCAACAGCTCC-3'
*Het-A*_RV 5'-AGCCAGCATTGCAGGTAGTT-3'

The Reference gene used was *RP49* (see below).

Total RNA extraction and RNA seq
Drosophila RNA was isolated from brain of third instar larvae exposed to four different irradiation treatments (non-pretreated control, 0.4 Gy chronic exposure, 10 Gy acute exposure, and 0.4 Gy + 10 Gy). Brains (100 brains/sample) were dissected in triplicate and RNA extracted using TRIzol (TRI Reagent® SIGMA Life Science, Sigma-Aldrich). The RNA-Seq of each individual sample was carried out from IGA Technology Services (Udine, Italy). cDNA libraries were constructed with 1 µg of total RNA by using the "Ovation® Drosophila RNA-Seq System" (TECAN-NuGEN, Redwood City, CA, USA) following the manufacturer's instructions. The total RNA was fragmented 3 min at 94 °C. 1X Agencourt AMPure XP beads (Agencourt Bioscience Cooperation, Beckman Coulter, Beverly, MA, USA). Total RNA samples and final cDNA libraries were quantified with the Qubit 2.0 Fluorometer (Invitrogen, Carlsbad, CA, USA) and quality tested by Agilent 2100 Bioanalyzer Nano assay. For cluster generation on the flow cell, libraries were processed with cBot (Illumina, San Diego, CA, USA) following the manufacturer's instructions. Sequencing was carried out in single-end mode (1×75 bp) by using NextSeq500 (Illumina) with a targeted sequencing depth of about 40 million reads per sample. Raw data were processed with the software CASAVA v1.8.2 (Illumina) for both format conversion and de-multiplexing. Resulting reads were then analyzed using the bcbio-nextgen pipeline (version 1.0.6). Specifically, reads were aligned against the Drosophila melanogaster reference genome (BDGP6) using STAR (v2.5.3a); gene abundances were estimated with Salmon (v0.9.1). Differential expression analysis at the gene level was performed using the DESeq2 R package. Genes with an adjusted p-value (FDR) <0.05 after correction for multiple testing (Benjamini-Hochberg method) were considered differentially expressed. lncRNAs polyA+ were also detected as the RNAseq library was polyA+ enriched. Finally, to analyze the functional relationships of these differentially expressed genes, a Gene Ontology (GO) functional enrichment analysis through the DAVID v. 6.8 web tool (https://david.ncifcrf.gov/,(Huang da et al., 2009)) was performed.

Sequence reads are available on NCBI BioProject database with the accession number SUB10002092

cDNA amplification and qPCR
To validate the expression levels of transcripts selected from the RNA seq analysis, equal amounts of cDNA were synthesized from 300 ng of total RNA for each sample by using the iScript™ cDNA Synthesis Kit (Bio-Rad, Hercules, CA, USA). Thirty nanograms of cDNA per reaction were analyzed for semi-qPCR using the SsoAdvanced™ Universal SYBR® Green Supermix Kit (Bio-Rad) following the manufacturer's protocol. The thermal cycling conditions were: 50 °C (2 min), 95 °C (10 min) followed by 40 cycles at 95 °C (15 s), 60 °C

(1 min), and 95 °C (15 s), 60 °C (1 min) 95 °C (15 s), and 60 °C (15 s). The specificity of the reaction was verified by melting curve analysis. The PCR primers used were:

LoqsRD_FW 5'-GCAAGGGCAAAAGCAAGAAGA-3'
LoqsRD_RV 5'-TTGAATGATACTCACTTCGCCCT-3'

LoqsRB_FW 5'-ACTGCTTAAGTTACAGAAGA-3'
LoqsRB_RV 5'-GGCCAGAGAAGGTCTTCTCC-3'

LoqsRA/RE_FW 5'-GTCTGCAGGAGACTCCCATC-3'
LoqsRA/RE_RV 5'-TCAAGCAAGTTTCGCCCTCC-3'

RP49 was amplified as a reference transcript using the following primers:

RP49_FW 5'-CCGCTTCAAGGGACAGTATCT-3'
RP49_RV 5'-ATCTCGCCGCAGTAAACGC-3'

PCR reactions were carried out in the ABI Prism 7300 System (Applied Biosystems, Foster City, CA, USA). Data processing was performed using the ABI SDS v2.1 software (Applied Biosystems). The critical threshold value was noted for each transcript and normalized to the internal control. The fold change was calculated using the comparative $2^{(-\Delta\Delta Ct)}$ method (Livak and Schmittgen, 2001).

Statistical analysis

Data were presented using the mean ± standard error (SE) obtained from, except for the EdU analysis, at least three independent experiments. All the statistical analyses were performed with Sigmaplot 11.0 (Systat Software, Imc., Chicago, IL, USA). The comparison between the two groups was analyzed by the Student t-test. The results were considered statistically significant when the *p* values were <0.05.

Acknowledgments
We are grateful to Prof. P.D Zamore (University of Massachusetts Medical School) for sharing all *loqs* transgenic flies. We thank P. Anello (ISS, Rome, Italy) for technical assistance with the γ irradiators. This work has been supported by grants from the Institute Pasteur of Paris (PTR-24-2017), and Institute Pasteur of Rome to GC, by grants from FERMI Institute for Multidisciplinary Studies (Cosmic Silence Project, Italy), INFN-CSN5 (RENOIR experiment) and ISS-INFN Operative Agreement for R&D activities in the field of Radiobiology to MAT

References

Belli, M., and Tabocchini, M.A. (2020). Ionizing Radiation-Induced Epigenetic Modifications and Their Relevance to Radiation Protection. Int J Mol Sci *21*.

Bosso, G., Cipressa, F., Moroni, M.L., Pennisi, R., Albanesi, J., Brandi, V., Cugusi, S., Renda, F., Ciapponi, L., Polticelli, F.*, et al.* (2019). NBS1 interacts with HP1 to ensure genome integrity. Cell Death Dis *10*, 951.

Cacchione, S., Cenci, G., and Raffa, G.D. (2020). Silence at the End: How Drosophila Regulates Expression and Transposition of Telomeric Retroelements. J Mol Biol *432*, 4305-4321.

Calabrese, E.J. (2015). On the origins of the linear no-threshold (LNT) dogma by means of untruths, artful dodges and blind faith. Environ Res *142*, 432-442.

Calabrese, E.J. (2017). The Mistaken Birth and Adoption of LNT: An Abridged Version. Dose Response *15*, 1559325817735478.

Cenci, G. (2009). Drosophila cell cycle under arrest: uncapped telomeres plead guilty. Cell Cycle *8*, 990-995.

Cenci, G., Ciapponi, L., and Gatti, M. (2005). The mechanism of telomere protection: a comparison between Drosophila and humans. Chromosoma *114*, 135-145.

Cenci, G., Ciapponi, L., Marzullo, M., Raffa, G.D., Morciano, P., Raimondo, D., Burla, R., Saggio, I., and Gatti, M. (2015). The Analysis of Pendolino (peo) Mutants Reveals Differences in the Fusigenic Potential among Drosophila Telomeres. PLoS Genet *11*, e1005260.

Cenci, G., Rawson, R.B., Belloni, G., Castrillon, D.H., Tudor, M., Petrucci, R., Goldberg, M.L., Wasserman, S.A., and Gatti, M. (1997). UbcD1, a Drosophila ubiquitin-conjugating enzyme required for proper telomere behavior. Genes Dev *11*, 863-875.

Cenci, G., Siriaco, G., Raffa, G.D., Kellum, R., and Gatti, M. (2003). The Drosophila HOAP protein is required for telomere capping. Nat Cell Biol *5*, 82-84.

Ciapponi, L., Cenci, G., Ducau, J., Flores, C., Johnson-Schlitz, D., Gorski, M.M., Engels, W.R., and Gatti, M. (2004). The Drosophila Mre11/Rad50 complex is required to prevent both telomeric fusion and chromosome breakage. Curr Biol *14*, 1360-1366.

Ciapponi, L., Cenci, G., and Gatti, M. (2006). The Drosophila Nbs protein functions in multiple pathways for the maintenance of genome stability. Genetics *173*, 1447-1454.

Cipressa, F., and Cenci, G. (2013). DNA damage response, checkpoint activation and dysfunctional telomeres: face to face between mammalian cells and Drosophila. Tsitologiia *55*, 211-217.

Council, N.R. (2006). Health Risks from Exposure to Low Levels of Ionizing Radiation: BEIR VII Phase 2 (Washington, DC: The National Academies Press).

Das, B., Saini, D., and Seshadri, M. (2009). Telomere length in human adults and high level natural background radiation. PLoS One *4*, e8440.

Doksani, Y., and de Lange, T. (2014). The role of double-strand break repair pathways at functional and dysfunctional telomeres. Cold Spring Harb Perspect Biol *6*, a016576.

Esposito, G., Anello, P., Pecchia, I., Tabocchini, M.A., and Campa, A. (2016). Facility for gamma irradiations of cultured cells at low dose rates: design, physical characteristics and functioning. Appl Radiat Isot *115*, 227-234.

Esposito, G., Campa, A., Pinto, M., Simone, G., Tabocchini, M.A., and Belli, M. (2011). Adaptive response: modelling and experimental studies. Radiation protection dosimetry *143*, 320-324.

Faghihi, M.A., and Wahlestedt, C. (2009). Regulatory roles of natural antisense transcripts. Nat Rev Mol Cell Biol *10*, 637-643.

Francia, S., Michelini, F., Saxena, A., Tang, D., de Hoon, M., Anelli, V., Mione, M., Carninci, P., and d'Adda di Fagagna, F. (2012). Site-specific DICER and DROSHA RNA products control the DNA-damage response. Nature *488*, 231-235.
Fukunaga, R., Han, B.W., Hung, J.H., Xu, J., Weng, Z., and Zamore, P.D. (2012). Dicer Partner Proteins Tune the Length of Mature miRNAs in Flies and Mammals. Cell *151*, 912.
Gao, M., Wei, W., Li, M.M., Wu, Y.S., Ba, Z., Jin, K.X., Li, M.M., Liao, Y.Q., Adhikari, S., Chong, Z.*, et al.* (2014). Ago2 facilitates Rad51 recruitment and DNA double-strand break repair by homologous recombination. Cell Res *24*, 532-541.
Gatti, M., Tanzarella, C., and Olivieri, G. (1974). Analysis of the chromosome aberrations induced by x-rays in somatic cells of Drosophila melanogaster. Genetics *77*, 701-719.
Giansanti, M.G., Bonaccorsi, S., Kurek, R., Farkas, R.M., Dimitri, P., Fuller, M.T., and Gatti, M. (2006). The class I PITP giotto is required for Drosophila cytokinesis. Curr Biol *16*, 195-201.
Hart, T., Tong, A.H.Y., Chan, K., Van Leeuwen, J., Seetharaman, A., Aregger, M., Chandrashekhar, M., Hustedt, N., Seth, S., Noonan, A.*, et al.* (2017). Evaluation and Design of Genome-Wide CRISPR/SpCas9 Knockout Screens. G3 (Bethesda) *7*, 2719-2727.
Hartig, J.V., Esslinger, S., Bottcher, R., Saito, K., and Forstemann, K. (2009). Endo-siRNAs depend on a new isoform of loquacious and target artificially introduced, high-copy sequences. EMBO J *28*, 2932-2944.
Huang da, W., Sherman, B.T., and Lempicki, R.A. (2009). Systematic and integrative analysis of large gene lists using DAVID bioinformatics resources. Nat Protoc *4*, 44-57.
Keskin, H., Meers, C., and Storici, F. (2016). Transcript RNA supports precise repair of its own DNA gene. RNA Biol *13*, 157-165.
Keskin, H., Shen, Y., Huang, F., Patel, M., Yang, T., Ashley, K., Mazin, A.V., and Storici, F. (2014). Transcript-RNA-templated DNA recombination and repair. Nature *515*, 436-439.
Korandova, M., Krucek, T., Szakosova, K., Kodrik, D., Kuhnlein, R.P., Tomaskova, J., and Capkova Frydrychova, R. (2018). Chronic low-dose pro-oxidant treatment stimulates transcriptional activity of telomeric retroelements and increases telomere length in Drosophila. J Insect Physiol *104*, 1-8.
Laurencon, A., Purdy, A., Sekelsky, J., Hawley, R.S., and Su, T.T. (2003). Phenotypic analysis of separation-of-function alleles of MEI-41, Drosophila ATM/ATR. Genetics *164*, 589-601.
Lim, M.Y., Ng, A.W., Chou, Y., Lim, T.P., Simcox, A., Tucker-Kellogg, G., and Okamura, K. (2016). The Drosophila Dicer-1 Partner Loquacious Enhances miRNA Processing from Hairpins with Unstable Structures at the Dicing Site. Cell Rep *15*, 1795-1808.
Lustig, A., Shterev, I., Geyer, S., Shi, A., Hu, Y., Morishita, Y., Nagamura, H., Sasaki, K., Maki, M., Hayashi, I.*, et al.* (2016). Long term effects of radiation exposure on telomere lengths of leukocytes and its associated biomarkers among atomic-bomb survivors. Oncotarget *7*, 38988-38998.
Luxton, J.J., McKenna, M.J., Lewis, A., Taylor, L.E., George, K.A., Dixit, S.M., Moniz, M., Benegas, W., Mackay, M.J., Mozsary, C.*, et al.* (2020a). Telomere Length Dynamics and DNA Damage Responses Associated with Long-Duration Spaceflight. Cell Rep *33*, 108457.
Luxton, J.J., McKenna, M.J., Taylor, L.E., George, K.A., Zwart, S.R., Crucian, B.E., Drel, V.R., Garrett-Bakelman, F.E., Mackay, M.J., Butler, D.*, et al.* (2020b). Temporal

Telomere and DNA Damage Responses in the Space Radiation Environment. Cell Rep *33*, 108435.
Madigan, J.P., Chotkowski, H.L., and Glaser, R.L. (2002). DNA double-strand break-induced phosphorylation of Drosophila histone variant H2Av helps prevent radiation-induced apoptosis. Nucleic Acids Res *30*, 3698-3705.
Malone, C.D., and Hannon, G.J. (2009). Small RNAs as guardians of the genome. Cell *136*, 656-668.
Marcus, C.S. (2016). Destroying the Linear No-threshold Basis for Radiation Regulation: A Commentary. Dose Response *14*, 1559325816673491.
Marques, J.T., Kim, K., Wu, P.H., Alleyne, T.M., Jafari, N., and Carthew, R.W. (2010). Loqs and R2D2 act sequentially in the siRNA pathway in Drosophila. Nat Struct Mol Biol *17*, 24-30.
Marques, J.T., Wang, J.P., Wang, X., de Oliveira, K.P., Gao, C., Aguiar, E.R., Jafari, N., and Carthew, R.W. (2013). Functional specialization of the small interfering RNA pathway in response to virus infection. PLoS Pathog *9*, e1003579.
Michalik, K.M., Bottcher, R., and Forstemann, K. (2012). A small RNA response at DNA ends in Drosophila. Nucleic Acids Res *40*, 9596-9603.
Morgan, W.F., and Bair, W.J. (2013). Issues in low dose radiation biology: the controversy continues. A perspective. Radiat Res *179*, 501-510.
Movahedi, A., Mostajaboddavati, M., Rajabibazl, M., Mirfakhraie, R., and Enferadi, M. (2019). Association of telomere length with chronic exposure to ionizing radiation among inhabitants of natural high background radiation areas of Ramsar, Iran. Int J Radiat Biol *95*, 1113-1121.
Nenoi, M., Wang, B., and Vares, G. (2015). In vivo radioadaptive response: a review of studies relevant to radiation-induced cancer risk. Human & experimental toxicology *34*, 272-283.
Olivieri, G., Bodycote, J., and Wolff, S. (1984). Adaptive response of human lymphocytes to low concentrations of radioactive thymidine. Science *223*, 594-597.
On, K., Crevel, G., Cotterill, S., Itoh, M., and Kato, Y. (2021). Drosophila telomere capping protein HOAP interacts with DSB sensor proteins Mre11 and Nbs. Genes Cells.
Raffa, G.D., Ciapponi, L., Cenci, G., and Gatti, M. (2011). Terminin: a protein complex that mediates epigenetic maintenance of Drosophila telomeres. Nucleus *2*, 383-391.
Raffa, G.D., Raimondo, D., Sorino, C., Cugusi, S., Cenci, G., Cacchione, S., Gatti, M., and Ciapponi, L. (2010). Verrocchio, a Drosophila OB fold-containing protein, is a component of the terminin telomere-capping complex. Genes Dev *24*, 1596-1601.
Raffa, G.D., Siriaco, G., Cugusi, S., Ciapponi, L., Cenci, G., Wojcik, E., and Gatti, M. (2009). The Drosophila modigliani (moi) gene encodes a HOAP-interacting protein required for telomere protection. Proc Natl Acad Sci U S A *106*, 2271-2276.
Saito, K., Ishizuka, A., Siomi, H., and Siomi, M.C. (2005). Processing of pre-microRNAs by the Dicer-1-Loquacious complex in Drosophila cells. PLoS Biol *3*, e235.
Seong, K.M., Kim, C.S., Seo, S.W., Jeon, H.Y., Lee, B.S., Nam, S.Y., Yang, K.H., Kim, J.Y., Kim, C.S., Min, K.J.*, et al.* (2011). Genome-wide analysis of low-dose irradiated male Drosophila melanogaster with extended longevity. Biogerontology *12*, 93-107.
Shibamoto, Y., and Nakamura, H. (2018). Overview of Biological, Epidemiological, and Clinical Evidence of Radiation Hormesis. Int J Mol Sci *19*.
Silva, E., Tiong, S., Pedersen, M., Homola, E., Royou, A., Fasulo, B., Siriaco, G., and Campbell, S.D. (2004). ATM is required for telomere maintenance and chromosome stability during Drosophila development. Curr Biol *14*, 1341-1347.
Slijepcevic, P. (2006). The role of DNA damage response proteins at telomeres--an "integrative" model. DNA Repair (Amst) *5*, 1299-1306.

Stecca, C., and Gerber, G.B. (1998). Adaptive response to DNA-damaging agents: a review of potential mechanisms. Biochemical pharmacology *55*, 941-951.
Tapio, S., and Jacob, V. (2007). Radioadaptive response revisited. Radiation and environmental biophysics *46*, 1-12.
UNSCEAR (2008). Sources and Effects of Ionizing Radiation, Vol I (United Nations).
Verdun, R.E., and Karlseder, J. (2006). The DNA damage machinery and homologous recombination pathway act consecutively to protect human telomeres. Cell *127*, 709-720.
Wei, W., Ba, Z., Gao, M., Wu, Y., Ma, Y., Amiard, S., White, C.I., Rendtlew Danielsen, J.M., Yang, Y.G., and Qi, Y. (2012). A role for small RNAs in DNA double-strand break repair. Cell *149*, 101-112.
Zhikrevetskaya, S., Peregudova, D., Danilov, A., Plyusnina, E., Krasnov, G., Dmitriev, A., Kudryavtseva, A., Shaposhnikov, M., and Moskalev, A. (2015). Effect of Low Doses (5-40 cGy) of Gamma-irradiation on Lifespan and Stress-related Genes Expression Profile in Drosophila melanogaster. PLoS One *10*, e0133840.
Zhou, R., Czech, B., Brennecke, J., Sachidanandam, R., Wohlschlegel, J.A., Perrimon, N., and Hannon, G.J. (2009). Processing of Drosophila endo-siRNAs depends on a specific Loquacious isoform. RNA *15*, 1886-1895.

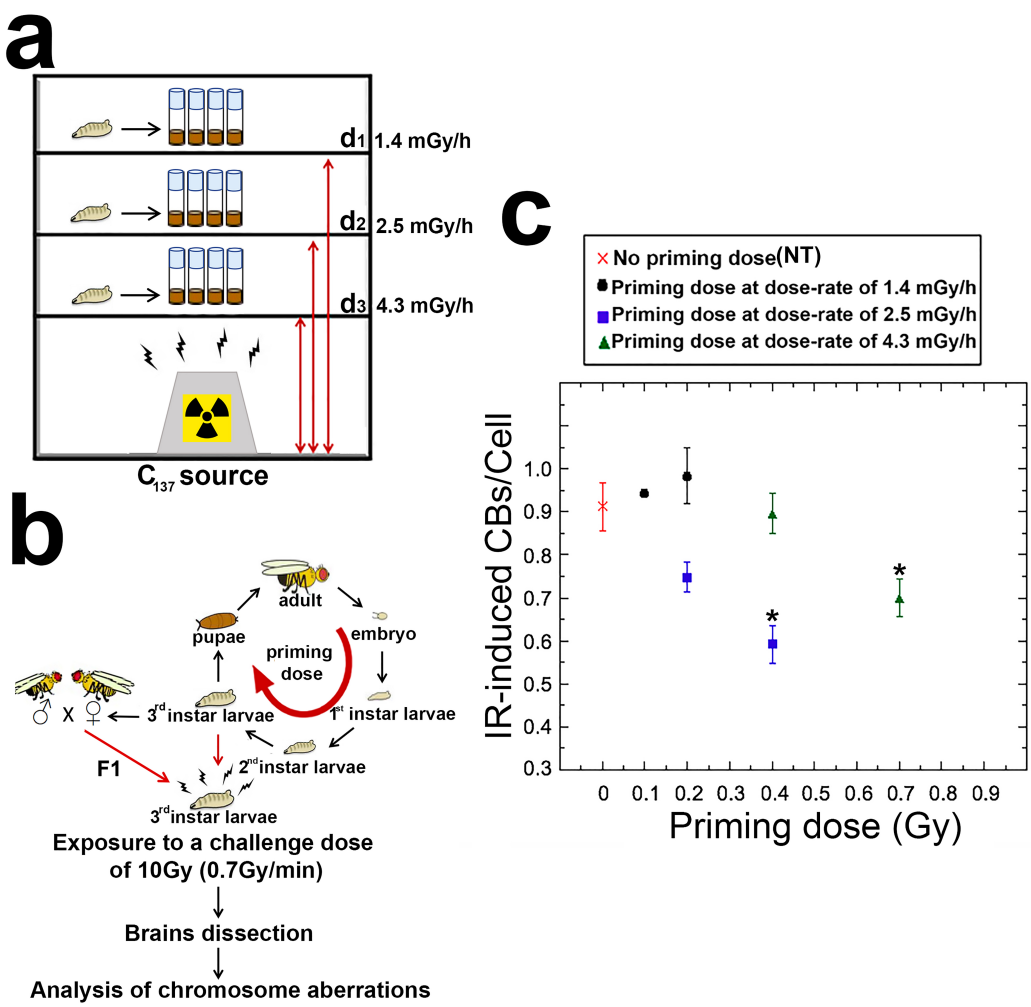

Figura 1

Figure 1. Experimental plan and analysis of CBs frequency in larval brains exposed to different irradiation treatments.
(a) Schematic representation of the LIBIS irradiator. The vials were placed at three different distances (d1, d2, and d3) from the ^{137}Cs source. **(b)** The priming dose was delivered during the embryos-larvae transition. The third instar larvae were collected and exposed to the challenging dose. Males and females pretreated during their development were crossed to obtain F_1. The third instar F_1 larvae were exposed to the challenge dose. Brains were then dissected to analyze the Chromosome Break (CBs) frequency. **(c)** The graph shows the average number of total CBs per cell induced by the challenge dose of 10Gy comparing different priming doses delivered at different dose-rates: no priming dose (red cross), 1.4mGy/h (solid circles), 2.5mGy/h (solid squares) and 4.3 mGy/h (solid triangles). At least three independent experiments were conducted. The comparisons were analyzed with Student t-test ($p<0.05$ (*).

a

PIR	Sex	γ-ray treatment	Total cells scored	ISOs/ Cell	CDs/ Cell	CBs/ Cell
–	♀	UNT	163	0.01±0.00	0.00±0.00	0.02±0.00
	♂	UNT	154	0.01±0.00	0.00±0.00	0.02±0.00
	♀	0.4Gy	116	0.01±0.01	0.00±0.00	0.02±0.01
	♂	0.4Gy	140	0.02±0.02	0.00±0.00	0.04±0.02
4h	♀	10Gy	552	0.39±0.04	0.30±0.06	1.08±0.05
	♂	10Gy	409	0.33±0.02	0.16±0.02	0.82±0.06
	♀	0.4Gy + 10Gy	970	0.20±0.04	0.20±0.02	0.60±0.02†
	♂	0.4Gy + 10Gy	418	0.16±0.02	0.21±0.07	0.53±0.08†
8h	♀	10Gy	572	0.14±0.01	0.24±0.02	0.52±0.03
	♂	10Gy	236	0.15±0.02	0.22±0.03	0.52±0.04
	♀	0.4Gy + 10Gy	332	0.15±0.02	0.17±0.02	0.47±0.03
	♂	0.4Gy + 10Gy	334	0.14±0.02	0.14±0.02	0.42±0.03
F_1 4h	♀	10Gy	1157	0.19±0.01	0.20±0.01	0.58±0.02†
	♂	10Gy	704	0.15±0.01	0.16±0.02	0.46±0.03†
F_2 4h	♀	10Gy	423	0.25±0.02	0.39±0.03	0.89±0.05
	♂	10Gy	288	0.18±0.03	0.47±0.04	0.83±0.05

b

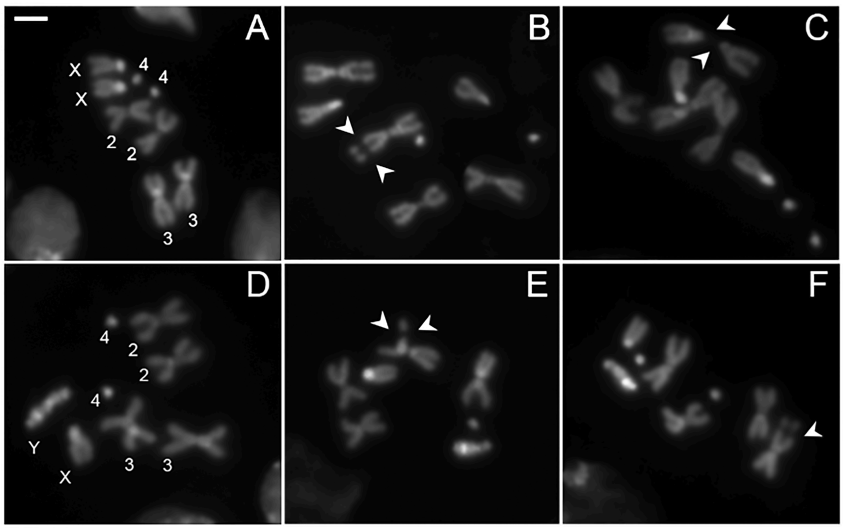

Figure 2

Figure 2. Effects of 0.4Gy LDDR treatment on CBs.
(a) Analysis of the frequency of CBs induced by the acute exposure to 10 Gy, in 0.4 Gy LDDR chronically treated and non-pretreated (NT) larvae after 4 and 8h post irradiation (PIR), and in the first and the second generation from adults exposed to 0.4Gy LDDR during their development. Chromosome exchanges did not vary and were not considered in the analysis. At least three independent experiments were conducted. LDDR: low dose/dose rate; ISOs: Isocromatid deletions; CDs: Chromatid deletions; CBs: chromosome breaks; PIR: post-irradiation time; F_1: first filial generation; F_2: second filial generation; †: statistically significant for $p<0.01$ (Student t-test). **(b)** Examples of IR-induced CBs in neuroblasts from O*regon*-R third instar larvae. (A) Wild type female and (D) male metaphases; (B) female and (C; F) male metaphases with examples of chromosome breaks (arrows); (E) male metaphase showing autosomal chromatid deletions (arrows). Bar= 5μm

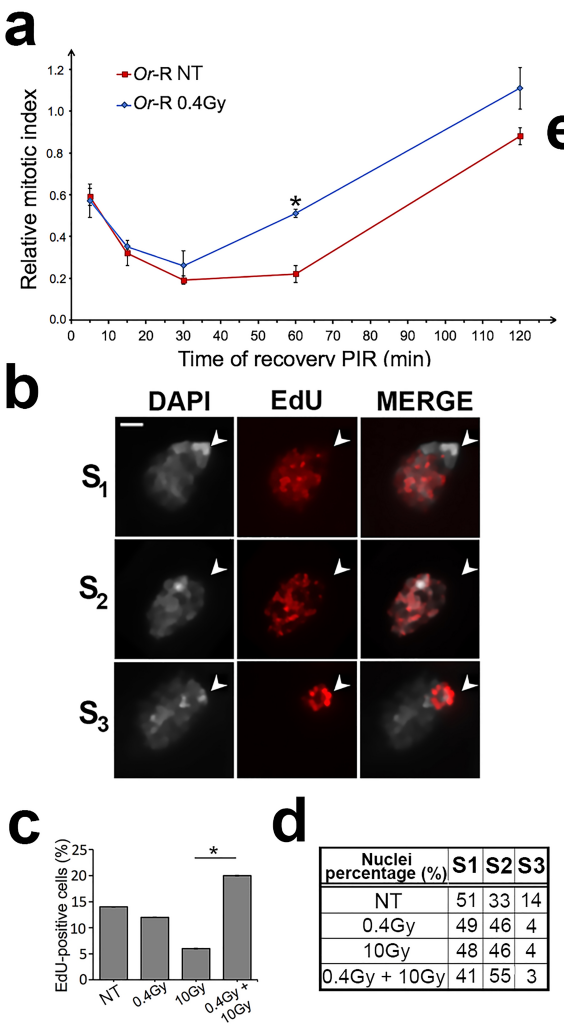

d

Nuclei percentage (%)	S1	S2	S3
NT	51	33	14
0.4Gy	49	46	4
10Gy	48	46	4
0.4Gy + 10Gy	41	55	3

e

Genotype	γ-ray treatment	Tot. cells scored	ISOs/ Cell	CDs/ Cell	CBs/ Cell
nbs[1]	NT	299	0.04±0.01	0.08±0.02	0.16±0.02
	0.4Gy	307	0.05±0.01	0.10±0.02	0.20±0.02
	2Gy	218	0.27±0.04	0.77±0.06	1.31±0.08
	0.4Gy + 2Gy	303	0.38±0.04	0.71±0.05	1.47±0.07
mre11[DC]	NT	153	0.06±0.02	0.14±0.03	0.26±0.04
	0.4Gy	195	0.09±0.02	0.17±0.03	0.35±0.04
	2Gy	325	0.25±0.03	0.61±0.04	1.11±0.06
	0.4Gy + 2Gy	296	0.22±0.03	0.42±0.04	0.86±0.05
rad50[Δ5.1]	NT	175	0.04±0.01	0.05±0.01	0.14±0.02
	0.4Gy	208	0.05±0.02	0.07±0.02	0.17±0.03
	2Gy	244	0.39±0.04	1.09±0.07	1.87±0.09
	0.4Gy + 2Gy	149	0.47±0.06	0.89±0.08	1.83±0.11
tefu[ATM6]	NT	194	0.02±0.01	0.07±0.02	0.11±0.02
	0.4Gy	251	0.04±0.01	0.04±0.01	0.12±0.02
	2Gy	278	0.42±0.04	0.04±0.01	0.88±0.06
	0.4Gy + 2Gy	301	0.24±0.03	0.03±0.01	0.49±0.04
mei41[29D]*/ATR*	NT	209	0.02±0.01	0.01±0.01	0.05±0.02
	0.4Gy	613	0.04±0.01	0.03±0.01	0.11±0.01
	5Gy	227	0.36±0.04	0.54±0.04	1.26±0.07
	0.4Gy + 5Gy	304	0.36±0.03	0.80±0.05	1.52±0.07
rad51[1]	NT	357	0.00±0.00	0.01±0.00	0.01±0.00
	0.4Gy	558	0.01±0.00	0.00±0.00	0.02±0.00
	10Gy	348	0.35±0.03	0.77±0.05	1.47±0.06
	0.4Gy + 10Gy	264	0.38±0.04	0.68±0.05	1.44±0.07
ligIV[5]	NT	197	0.05±0.02	0.20±0.03	0.30±0.04
	0.4Gy	179	0.05±0.02	0.17±0.03	0.27±0.04
	10Gy	491	0.36±0.03	0.26±0.02	0.98±0.04
	0.4Gy + 10Gy	472	0.24±0.02	0.24±0.02	0.72±0.04
ATPCL[DG23]	NT	159	0.01±0.01	0.14±0.03	0.16±0.03
	0.4Gy	150	0.05±0.02	0.09±0.02	0.19±0.04
	10Gy	442	0.26±0.02	0.48±0.03	1.00±0.05
	0.4Gy + 10Gy	214	0.13±0.02	0.27±0.04	0.53±0.05†

Figure 3

Figure 3. The influence of cell cycle and DDR on the RAR.
(a) Checkpoint assay of *Oregon*-R 0.4Gy LDDR chronically exposed O*regon*-R larval brains versus non-pretreated controls. In the picture is shown the relative mitotic index (MI) calculated as the ratio between the MI of each irradiation treatment and the MI of non-pretreated *Oregon*-R wild type. Note that the relative MI of 0.4Gy LDDR larvae increases after 60 minutes post-irradiation compared to non-pretreated control. At least three independent experiments were repeated. Values of $p<0.05$ (*) were considered as statistically significant (Student t-test). **(b)** EdU incorporation analysis of *Oregon*-R larval brain cells exposed to IR. EdU-positive cell nuclei of larval brains show 3 different incorporation patterns: S_1 represents early S phase nuclei that do not incorporate Edu in the DAPI-stained chromocenter; S_2 represents mid-S phase nuclei that incorporate EdU in all DAPI-stained nucleus; S_3 shows nuclei in the late S-phase that incorporate EdU only in

the chromocenter. **(c)** Frequencies of EdU positive nuclei. The frequencies of EdU positive nuclei in each sample (NT, 0.4 Gy LDDR, 10 Gy, 0.4 Gy LDDR + 10 Gy) were obtained by examining at least 2000 nuclei from at least 2 brains. Values of $p<0.01$ (*) were considered as statistically significant (Student t-test). **(d)** Quantification (%) of EdU positive cells divided in S1, S2, and S3 phases according to the staining pattern observed in **(b)**. No statistical differences were observed in treated cells compared to controls. **(e)** DNA repair gene mutant larvae do not elicit RAR. Frequency of CBs induced by an acute 2 Gy, 5 Gy or 10 Gy irradiation on 0.4 Gy LDDR-pretreated *Drosophila* strains mutated in genes involved in the DNA damage response (DDR). The *ATPCL* mutant was used as a control. Note that in all DNA repair (but not in *ATPCL*) mutants RAR is abolished. ISOs: isochromatid deletions; CDs: chromatid deletions; CBs: chromosome breaks; NT: non-pretreated; PIR: post-irradiation time; †: $p<0.01$ (Student t-test). Bar= 10μm

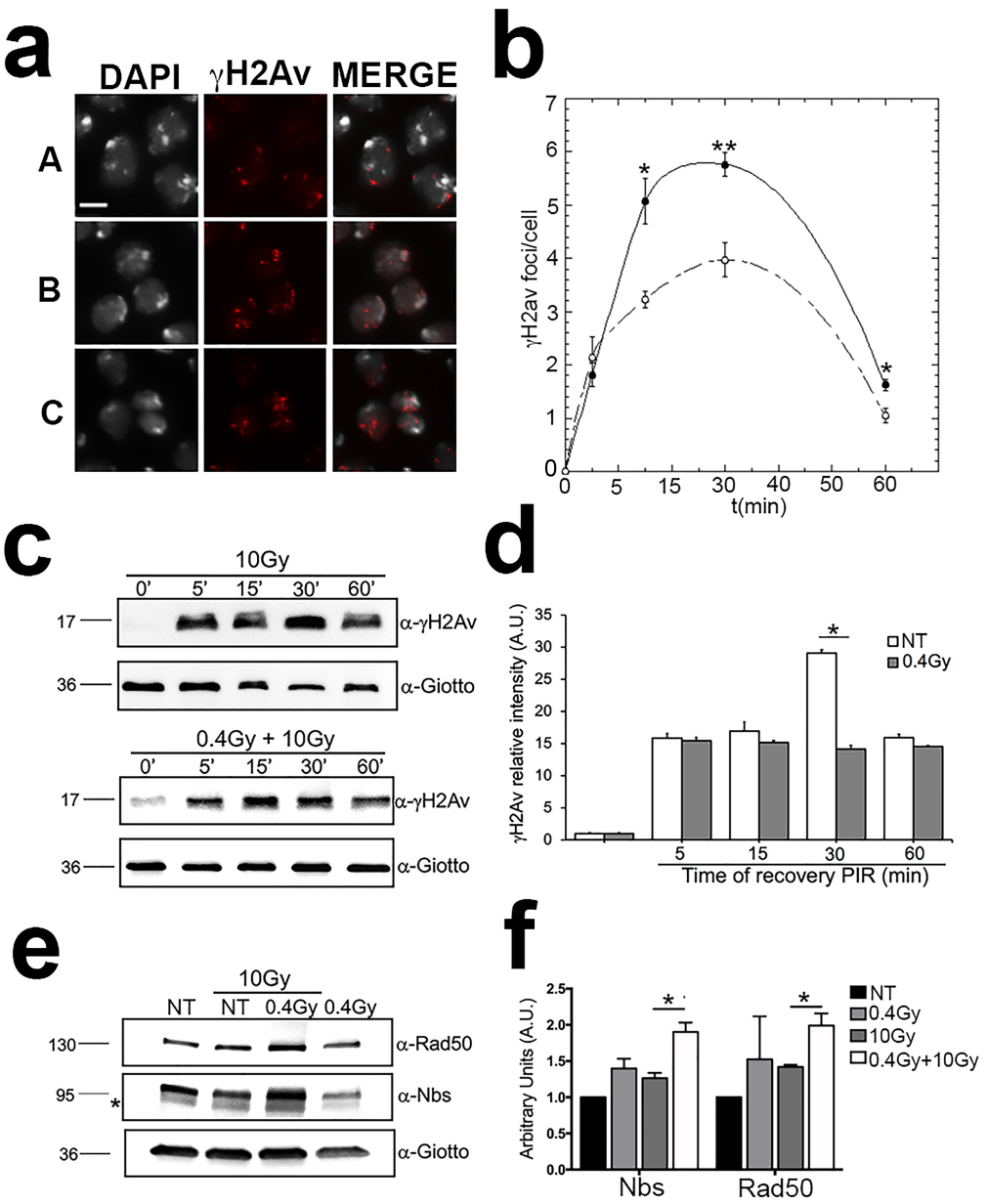

Figure 4

Figure 4. DNA damage accumulation in 0.4 Gy LDDR -pretreated and non-pretreated larval brains.
(a) Anti γH2Av immunofluorescence on 10 Gy irradiated cells showing (A) low damage (0-3 γH2Av spots per cell); (B) medium damage (4-7 γH2Av spots per cell); (C) high damage (> 7 γH2Av spots per cell **(b)** Quantification of γH2Av foci/cell at different PIR time points; NT: non-pretreated **(c)** Western Blot analysis of γH2Av levels in treated and non-pretreated brains at 5 min, 15 min, 30 min, and 60 min PIR after acute IR exposure of 10 Gy. Giotto (VIB) was used as a loading control. **(d)** Quantification of γH2Av signals from the WB analysis. Three independent WBs were used for the quantification. (*p<0.05; Student t-test); PIR: post-irradiation times. **(e)** Western Blot analysis of Nbs and Rad50 levels in treated and non-pretreated brains after acute IR exposure of 10 Gy. Giotto (VIB) was used as a loading control. **(f)** Quantification of Nbs and Rad50 signals from the WB analysis. NT: non-pretreated. Bar= 10μm

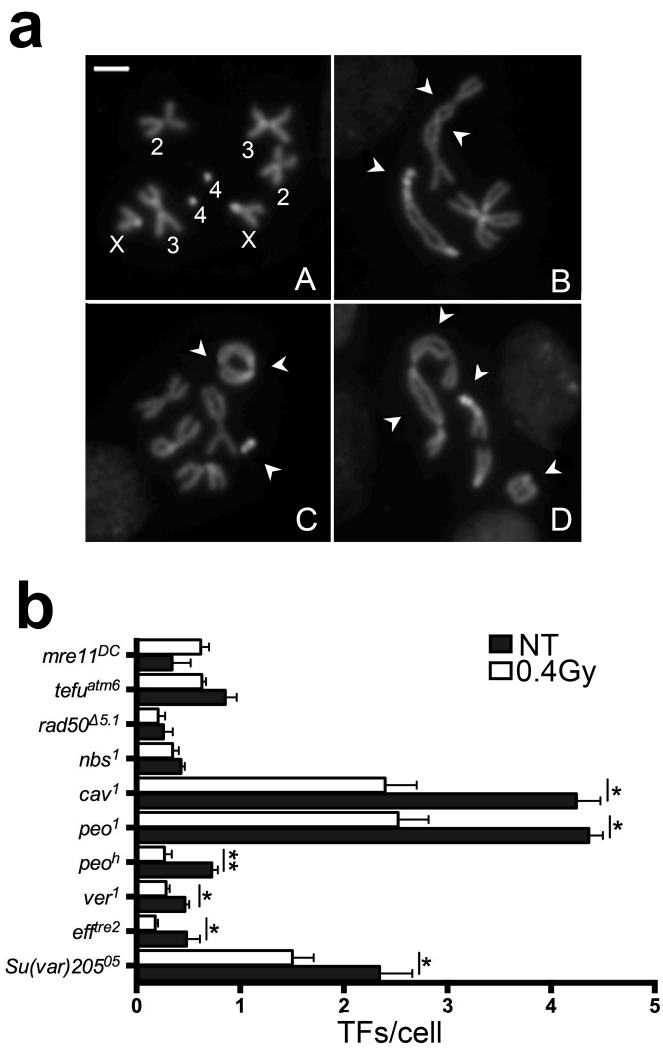

Figure 5

Figure 5. Analysis of TFs frequency in telomere capping and DDR mutants exposed to 0.4 Gy LDDR.
(a) Examples of TFs scored for the TF frequency analysis. **(**A) Female wild-type metaphase; (B) female metaphase showing a Double Telomere Association (DTA) between the chromosomes 2 (arrows), a DTA involving both chromosomes 4 and both chromosomes X (arrows); (C) female metaphase showing a ring consisting of both X chromosomes (arrows) and a DTA between the chromosomes 4 (arrow); (D) female metaphase showing a multicentric chromosome configuration involving 3DTAs, a DTA between chromosome 4 and XR and a ring chromosome (arrows). **(b)** TF frequency (DTAs only) in 0.4 Gy LDDR-pretreated and non-pretreated *Drosophila* strains mutated in genes encoding telomeric proteins (*ver*, *cav*, *eff*, *Su(var)205*, and *peo*) or DNA damage repair factors (*rad50*, *mre11*, *nbs*, and *tefu*). (**p*<0.05; ***p*<0.01). DTAs: double telomere associations; NT: non-pretreated. Bar= 5μm

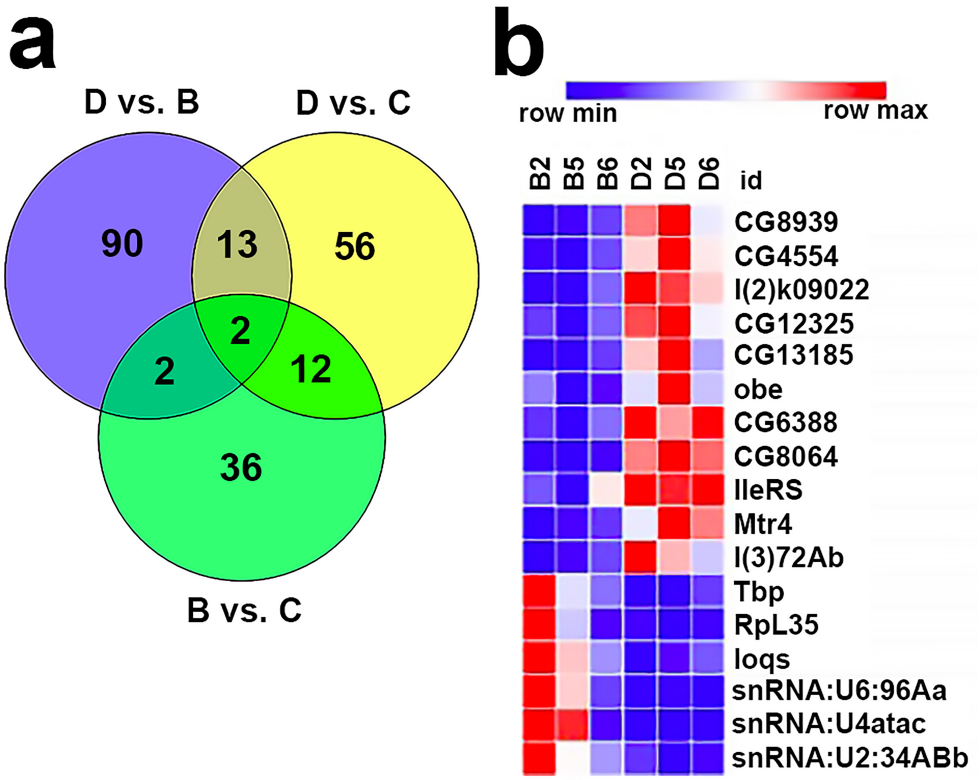

Figure 6

Figure 6. Analysis of differentially expressed genes in radio adaptive response. **(a)** Representation of the Venn diagram including all differentially expressed genes from 0.4 Gy LDDR + 10 Gy *vs*. 10 Gy (D *vs*. B), 0.4 Gy LDDR + 10 Gy *vs*. 0.4 Gy LDDR (D *vs*. C) and 10 Gy *vs*. 0.4 Gy LDDR (B *vs*. C) comparisons. Only a very low percentage of genes were in common among all comparisons. **(b)** Heat map representing the differentially expressed genes from 0.4 Gy LDDR + 10 Gy *vs*. 10 Gy (D *vs*. B) comparison belonging to "RNA processing" biological process obtained from DAVID functional enrichment analysis. A color-coded scale for the normalized expression values is used: red and blue represent high and low expression levels. A complete list of differentially expressed genes is provided in the Supplementary Materials (Tables 4-8).

a

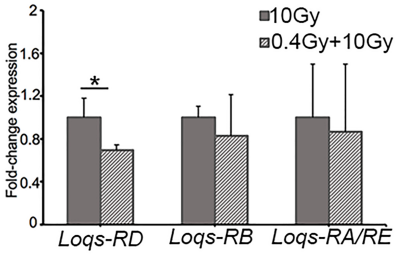

b

	γ-ray treatment	Total cells scored	ISOs/ Cell	CDs/ Cell	CBs/ Cell
Or-R	10Gy	324	0.36±0.03	0.29±0.02	1.01±0.05
loqs^{KO} /loqs^{KO}	NT	497	0.00±0.00	0.02±0.01	0.02±0.01
	0.4Gy	339	0.01±0.00	0.02±0.01	0.04±0.01
	10Gy	561	0.13±0.02	0.14±0.02	0.40±0.03†
	0.4Gy + 10Gy	679	0.22±0.02	0.16±0.02	0.60±0.03†
loqs^{KO}/+	10Gy	211	0.16±0.03	0.21±0.03	0.53±0.05†
	0.4Gy + 10Gy	305	0.21±0.03	0.15±0.02	0.56±0.04†
loqs^{KO};[loqs-PD]	10Gy	175	0.27±0.04	0.58±0.06	1.12±0.08
	0.4Gy + 10Gy	85	0.15±0.04	0.42±0.07	0.72±0.09
loqs^{KO};[loqs-PB]	10Gy	133	0.14±0.03	0.26±0.04	0.54±0.06†
	0.4Gy + 10Gy	97	0.12±0.04	0.26±0.05	0.50±0.07†

c

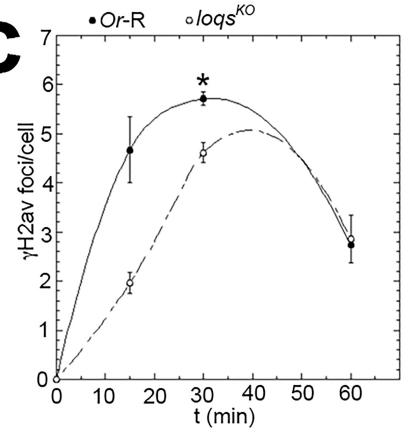

d

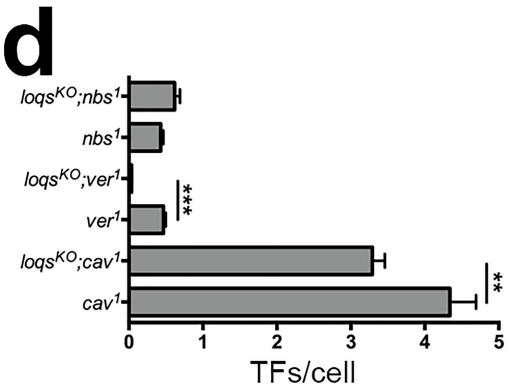

Figure 7

Figure 7. Loqs as a RAR responsive factor.
(a) RT-qPCR on different *Loqs* splicing variants. *Loqs-RD* (but not *-RB*, *-RA*, and *-RE*) transcripts are downregulated in 0.4 Gy LDDR-pretreated male brains following the exposure to 10 Gy. Three different experiments were performed. The statistical analysis used was Student t-test (*p<0.05). **(b)** Frequency of IR-induced CBs in 0.4Gy LDDR

treated and non-pretreated (NT) homozygous and heterozygous *Loqs*^{KO} mutants as well as *OR*-R controls, in *loqs*^{KO} null mutants expressing the Loqs-PD and Loqs-PB exogenous isoforms. ISOs: isochromatid breaks; CDs: chromatid deletions; CBs: chromosome breaks; †: statistically significant using Student t-test ($p<0.05$). **(c)** Kinetics of γH2Av recruitment after irradiation with 10 Gy in *loqs*^{KO} mutants. PIR: post irradiation times; NT: non-pretreated. **(d)** The graph shows the TFs (revealed by counting only DTAs) in *loqs;ver*, *loqs;cav* and *loqs*;*nbs*^{1} double mutants as well in *ver, cav* and *nbs* single mutants. The statistical analysis was performed by Student t-test (*$p<0.05$; **$p<0.01$). DTAs: double telomere associations.